A Potential Iron Pharmaceutical Composition for the Treatment of Iron-deficiency Anaemia. The Crystal and Molecular Structure of *mer*-Tris-(3-hydroxy-2-methyl-4*H*-pyran-4-onato)iron(III)†

Mustafa T. Ahmet, Christopher S. Frampton, and Jack Silver*
Department of Chemistry, University of Essex, Wivenhoe Park, Colchester CO4 3SQ

mer-Tris(3-hydroxy-2-methyl-4*H*-pyran-4-onato)iron(III) has potential use in the treatment of iron-deficiency anaemia. It displays the ideal properties that a new iron chelation complex must possess to be an effective treatment. These properties are discussed. The crystal and molecular structure of this complex has been determined from single-crystal *X*-ray diffraction data and refined by least squares to $R = 0.0649$ for 2 735 independent reflections. The compounds crystallizes in the monoclinic space group $P2_1/c$ with cell dimensions $a = 7.369(1)$, $b = 14.720(3)$, and $c = 19.964(5)$ Å, $\beta = 100.41(2)°$, and $Z = 4$. The iron atom lies in a distorted octahedral environment with the three ligands bonded through the hydroxy and ketone oxygen atoms to give the *mer* configuration. Variable-temperature ^{57}Fe Mössbauer data for the complex are reported and the results are discussed in relation to the structure.

An adequate supply of iron in the diet of man and animals is an essential requisite for tissue growth. Even though there is usually an ample amount of iron in the diet, the level of absorption of this element from food is generally low. The result is that the supply of iron to the body can easily become critical under a variety of conditions. Iron-deficiency anaemia is commonly encountered in pregnancy and also may be a problem in the newly born, particularly in animal species such as the pig. In certain pathological conditions there is a poor distribution of body iron leading to a state of chronic anaemia, *e.g.* in chronic diseases such as rheumatoid arthritis, certain haemolytic diseases, and cancer.

There have been a great many preparations for the treatment of iron-deficiency anaemia, almost all of which are complexes of iron(II), *e.g.* the sulphate, fumarate, and gluconate. Iron(II) sulphate is often preferred as it is the cheapest form and is at least as effective as any other. The predominant reason for the choice of iron(II) over iron(III) complexes is their increased solubility in the range pH 3—7 (solubility being an essential property in the permeation of membranes). Iron(II) complexes do, however, have a major disadvantage in that they are very sensitive to oxidation, especially in aqueous environments. This can be initially hindered by protectively coating iron(II) preparations (in tablet form) in some way. However, on dissolving within the gut, oxidation will still occur; insoluble iron(III) salts (containing hydroxides) result, which frequently cause irritation and gastro-intestinal stress. Such conditions are severe because, to ensure enough iron is absorbed even after this precipitation, large doses are necessary (average dose 200 mg per day for an average 70-kg adult).[1]

Obviously, soluble iron(III) complexes would thus be preferred (as oxidation would not be a problem). Such complexes however are likely to be charged (unsatisfactory for passive membrane diffusion). If they were neutral they may still be toxic.

From this discussion clearly the ideal properties a new iron chelation complex for treating iron-deficiency anaemia would possess[2] are that, (*a*) the complex has a high affinity for iron(III), (*b*) the resultant iron(III) complex is neutral, (*c*) the complex is soluble in the range pH 6—9, and (*d*) the complex is non-toxic. In addition after absorption into the body it must enter into an equilibrium with transferrin so that the iron is available for utilization in metabolic pathways. To achieve this latter condition it is necessary that the chelator is rapidly metabolized so that the iron is freely available.[3–8]

One such compound is that formed between iron and 3-hydroxy-2-methyl-4*H*-pyran-4-one (HL, maltol). The stability constant for [FeL_3] has been reported[9] as 28.5 compared to 36 for apotransferrin,[10] and although it would dissociate below pH 4 to form the charged 1:1 and 1:2 iron(III):maltol species with free ligand (in the stomach for instance) the 3:1 species should reassemble under neutral to alkaline conditions such as those found in the small intestine.[11]

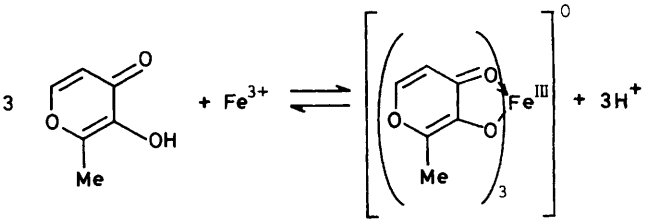

A number of related molecules to maltol are the 3-hydroxy-4-pyrones[3] and the 3-hydroxy-2-pyrones.[3] All these ligands are water soluble. Delocalization of the lone pair of electrons of the ring oxygen or nitrogen will result in each of these molecules gaining some aromatic character. Because of this potential for aromaticity the hydroxyl groups have low pK_a values (8.68 in water).[12]

Recently [FeL_3] and similar complexes have been shown to possess the desirable properties outlined above for the treatment of iron-deficiency-linked diseases.[3–8] Maltol has been tested on the rat, mouse, and dog, and toxicity studies have all proved negative.[13,14] Metabolism studies of maltol on the dog have been interpreted to show that elimination is rapid and extentsive. Because of these facts and the similarity of maltol to other chelator molecules,[3] the crystal structure of [FeL_3] and the electronic structure around the iron(III) centre were studied with the aim of pinpointing factors that may influence the iron binding in this complex. We also report ^{57}Fe Mössbauer data.

Results and Discussion

The Structure of mer-*Tris*(3-*hydroxy*-2-*methyl*-4H-*pyran*-4-*onato*)*iron*(III), [FeL_3].—The unit cell of the crystal contains

---

† *Supplementary data available:* see Instructions for Authors, *J. Chem. Soc., Dalton Trans.*, 1988, Issue 1, pp. xvii—xx.

four discrete molecules with no unusual intermolecular contacts. The two *mer*-Λ isomers are related to the two *mer*-Δ isomers by the centre of symmetry. Table 1 lists the atomic co-ordinates. Table 2 the individual bond lengths and angles.

The Figure[15] shows a view of the *mer*-Λ isomer with the atom-numbering scheme. The iron atoms lie in a trigonally distorted octahedral environment co-ordinated to the hydroxy and ketone oxygen atoms of three ligands in the *mer* configuration, this being the statistically most probable configuration and is the same as that found for the aluminium derivative.[16] The molecule exhibits the expected propeller shape; the angle of trigonal twist is 50.43°, *cf.* 60° for a regular octahedron and 0° for trigonal prismatic co-ordination. In each case it can be seen that the ligands are essentially planar.

The distortion of the octahedral environment is primarily due

Table 1. Positional parameters for [FeL$_3$] with standard errors in parentheses

Atom	*x*	*y*	*z*
Fe	3 337.1(9)	98.4(4)	6 976.4(4)
O(11)	3 524(4)	1 022(2)	7 721(1)
O(12)	6 119(4)	388(2)	7 086(1)
C(11)	5 278(6)	1 253(3)	7 944(2)
C(12)	6 623(6)	898(3)	7 594(2)
C(13)	8 539(6)	1 143(4)	7 843(3)
C(14)	8 880(7)	1 704(5)	8 371(3)
C(15)	5 793(6)	1 835(4)	8 492(3)
C(16)	4 574(7)	2 278(4)	8 894(3)
O(13)	7 611(5)	2 059(3)	8 699(2)
O(21)	2 304(4)	1 012(2)	6 274(1)
O(22)	3 527(4)	9 383(2)	6 082(1)
C(21)	2 257(6)	729(3)	5 630(2)
C(22)	2 913(6)	9 841(3)	5 540(2)
C(23)	2 857(6)	9 523(4)	4 851(3)
C(24)	2 177(6)	72(5)	4 321(3)
C(25)	1 598(6)	1 259(4)	5 065(2)
C(26)	859(8)	2 148(5)	5 061(3)
O(23)	1 595(5)	892(3)	4 413(2)
O(31)	4 018(4)	9 031(2)	7 596(2)
O(32)	758(4)	9 638(2)	7 055(1)
C(31)	2 532(6)	8 630(3)	7 753(2)
C(32)	798(6)	8 963(3)	7 451(2)
C(33)	9 161(7)	8 520(4)	7 607(3)
C(34)	9 441(7)	7 807(4)	8 040(4)
C(35)	2 664(7)	7 939(4)	8 246(3)
C(36)	4 368(7)	7 577(4)	8 641(3)
O(33)	1 067(5)	7 550(2)	8 376(2)

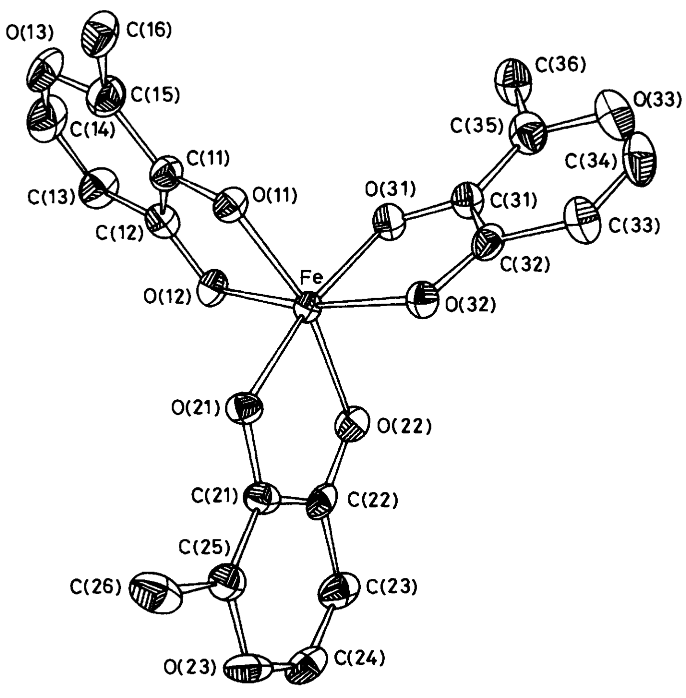

Figure. Molecular structure of [FeL$_3$] showing the atom numbering scheme

Table 2. Bond lengths (Å) and angles (°) for [FeL$_3$] with estimated standard deviations in parentheses

(*i*) Iron co-ordination

Fe–O(11)	1.986(4)	Fe–O(12)	2.068(3)
Fe–O(21)	1.978(3)	Fe–O(22)	2.076(4)
Fe–O(31)	1.996(4)	Fe–O(32)	2.050(4)
O(11)–Fe–O(12)	81.2(1)	O(11)–Fe–O(22)	165.1(2)
O(21)–Fe–O(22)	80.2(2)	O(21)–Fe–O(31)	169.7(1)
O(31)–Fe–O(32)	80.1(1)	O(12)–Fe–O(32)	167.4(1)

(*ii*) Ring 1

O(11)–C(11)	1.333(6)	C(14)–O(13)	1.335(8)
O(12)–C(12)	1.251(6)	O(13)–C(15)	1.369(6)
C(11)–C(12)	1.406(7)	C(15)–C(11)	1.376(8)
C(12)–C(13)	1.453(7)	C(15)–C(16)	1.453(8)
C(13)–C(14)	1.315(9)		
Fe–O(11)–C(11)	110.5(3)	C(13)–C(14)–O(13)	125.2(5)
Fe–O(12)–C(12)	110.7(3)	C(14)–O(13)–C(15)	119.7(5)
C(12)–C(11)–C(15)	119.8(5)	O(13)–C(15)–C(11)	120.0(5)
C(11)–C(12)–C(13)	118.1(5)	C(11)–C(15)–C(16)	126.5(5)
C(12)–C(13)–C(14)	117.2(5)	O(13)–C(15)–C(16)	113.5(5)
O(11)–C(11)–C(12)	118.5(5)	O(12)–C(12)–C(11)	118.3(5)
O(12)–C(12)–C(13)	123.5(5)	O(11)–C(11)–C(15)	122.0(5)

(*iii*) Ring 2

O(21)–C(21)	1.328(6)	C(24)–O(23)	1.303(8)
O(22)–C(22)	1.274(7)	O(23)–C(25)	1.391(7)
C(21)–C(22)	1.416(8)	C(25)–C(21)	1.372(8)
C(22)–C(23)	1.426(8)	C(25)–C(16)	1.419(10)
C(23)–C(24)	1.345(9)		
Fe–O(21)–C(21)	113.1(3)	C(23)–C(24)–O(23)	122.4(6)
Fe–O(22)–C(22)	111.8(3)	C(24)–O(23)–C(25)	122.8(5)
C(22)–C(21)–C(25)	120.1(5)	O(23)–C(25)–C(21)	117.9(6)
C(21)–C(22)–C(23)	118.1(5)	C(21)–C(25)–C(26)	127.5(6)
C(22)–C(23)–C(24)	118.7(6)	O(22)–C(22)–C(21)	117.7(5)
O(21)–C(21)–C(22)	117.3(5)	C(26)–C(25)–O(23)	114.6(5)
O(22)–C(22)–C(23)	124.4(6)	O(21)–C(21)–O(25)	122.6(3)

(*iv*) Ring 3

O(31)–C(31)	1.328(6)	C(34)–O(33)	1.315(7)
O(32)–C(32)	1.257(7)	C(33)–C(35)	1.373(7)
C(31)–C(32)	1.399(7)	C(35)–C(31)	1.397(8)
C(32)–C(33)	1.451(8)	C(35)–C(36)	1.452(8)
C(33)–C(34)	1.347(9)		
Fe–O(31)–C(31)	111.4(3)	C(33)–C(34)–O(33)	124.2(5)
Fe–O(32)–C(32)	113.0(3)	C(34)–O(33)–C(35)	121.5(5)
C(32)–C(31)–C(35)	119.7(5)	O(33)–C(25)–C(31)	118.6(5)
C(31)–C(32)–C(33)	118.9(5)	C(31)–C(35)–C(36)	125.7(5)
C(32)–C(33)–C(34)	116.6(5)	C(36)–C(35)–O(33)	115.9(5)
O(31)–C(31)–C(32)	118.5(5)	O(32)–C(32)–C(31)	117.2(5)
O(32)–C(32)–C(33)	123.9(5)	O(31)–C(31)–C(35)	121.9(5)

Table 3. Crystal structure data relevant to this work

Compound[a]	Fe–O bond distance (range)/Å	Ligand bite angle/°	Trigonal twist angle[b]/°	Ref.
(**1**) $[C_5H_{12}N]_3[Fe(C_6H_4O_2)_3]\cdot 1.5H_2O$	1.993(2)—2.037(2)	80.3(1)—82.1(1)	46.5(8)	17
(**2**) $K_3[Fe(C_6H_4O_2)_3]\cdot 1.5H_2O$	1.996(3)—2.035(6)	81.13(22)—81.37(22)	44.7(10)	18
(**3**) $[C_5H_{12}N]_3[\{Fe(C_6H_4O_2)_2\}_2(O_2CMe)]$	1.95(3)—2.03(2)	82.3(9), 84.0(4)	*c*	19
(**4**) $[Fe(nta)(dbc)]^{2-}$	1.887(3), 1.979(3)	*c*	*c*	20
(**5**) $[C_5H_{12}N]_2[Fe\{2,3\text{-}(O)_2\text{-}C_6H_3CONHCH_2CO_2Et\}_2(acac)]\cdot thf$	2.00—2.04	79.8, 80.2, 87.1	*c*	21
(**6**) $[Fe(acac)_3]$	1.986—2.004	86.7—87.3	56.6[d]	22
(**7**) $[Fe(acac)_3]\cdot AgClO_4\cdot H_2O$	1.97(1), 2.02(1)	86.4(4)—89.3(5)	*c*	23
(**8**) $[Fe(trop)_3]$	2.008	77.8	32.4[d]	24
(**9**) $[FeL'_3]$	2.008(1)	78.63(5)	36.6	25
(**10**) $[FeL''_3]$	2.016(1)	80.85(5)	42.1	25
(**11**) $[FeL_3]$	1.978(3)—2.076(4)	80.1(1)—81.2(1)	50.43	This work

[a] nta = Nitrilotriacetate(3 –), dbc = 3,5-di-t-butylcatecholate(2 –), acac = acetylacetonate, trop = tropolonate(1 –) = 2-hydroxycyclohepta-2,4,6-trien-1-onate, L′ = 1-hydroxy-2-pyridonate(1 –), L″ = 3-hydroxy-2-pyridonate(1 –), $C_6H_4O_2$ = catecholate(2 –), $C_5H_{12}N$ = piperidinium. [b] 60° for regular octahedron and 0° for trigonal prismatic co-ordination. [c] Not given. [d] Value taken as twice that in ref. 26.

Table 4. ^{57}Fe Mössbauer data for $[FeL_3]$[a]

T/K	Isomer shift[b]	Quadrupole splitting[b]	Contribution (%)
300	−0.14	0.19	5.5
	0.26	2.30	94.5
77	−0.04	0.19	20.7
	0.61	3.87	79.3
4	0.04	0.85	17.4
	0.57	4.54	82.6
77[c]	−0.16	0.97	59.1
	1.11	1.38	40.9

[a] Spectra are each fitted to two singlets. [b] Values in mm s^{-1} relative to natural iron foil (±0.01 mm s^{-1}). [c] Parameters for crystalline sample.

to the differences found in the iron–oxygen bond lengths, mean Fe–O(keto) and Fe–O(hydroxy) 2.065 and 1.987 Å respectively. The forces resulting in these differences are not immediately clear, though inter-ligand repulsion and packing forces must play a part.[17–26] When these values are compared to those of other similar tris chelate iron(III) complexes (Table 3) the following facts emerge: (*a*) the Fe–O bond lengths show a larger range of differences from those of other five-membered chelate rings [compounds (**1**)—(**5**), (**8**)—(**10**)], whereas the ligand bite angles are similar to those of the catechol complexes (**1**)—(**5**); (*b*) the trigonal twist angle of 50.43° is larger than those found in the other five-membered rings and (*c*) six-membered rings have larger bite angles (as expected) but smaller Fe–O distances.

The evidence of (*a*) and (*c*) taken together indicates that even allowing for packing and interligand repulsion effects, the mean Fe–O(keto) and Fe–O(hydroxy) bonds are significantly different. One likely explanation is that the methyl group *ortho* to the O(hydroxy), and the ring oxygen *para* to the O(keto) both exert differing σ and π electronic effects causing the asymmetry in the Fe–O bonding. This is in good agreement with that which is found for the aluminium derivative[15] and is in fact more obvious in $[FeL_3]$, possibly since the present structure does not suffer from any ligand disorder.

Bond valencies $\{S = \exp[(r_0 - r)/B]$; r = bond length, r_0 and B are empirically determined parameters)} calculated for the individual Fe–O bonds using the bond valence parameters determined by Brown and Altermatt[27,28] give mean values of S = 0.540 and 0.438 for Fe–O(hydroxy) and Fe–O(keto) respectively, which is consistent with the structure depicted for $[FeL_3]$. These differences consequently lower the *cis*-O–Fe–O bond angles below 90° (mean 80.5°).

^{57}Fe *Mössbauer Spectroscopy*.—Variable-temperature ^{57}Fe Mössbauer data for $[FeL_3]$ are presented in Table 4. The spectrum may be considered to consist of an asymmetric singlet which broadens with decreasing temperature. This observed line shape is characteristic of a tris(β-diketonato)iron(III) complex and has been attributed to paramagnetic relaxation effects arising from incomplete relaxation of electronic spins.[29–31]

The overall relaxation rate may be expressed as a sum of the spin–spin and spin–lattice relaxation rates. It has been shown that for high-spin ($S = \frac{5}{2}$) iron(III) species the spin–spin contribution to the relaxation rate predominates and that the spin–spin interaction decreases as the iron–iron spacing increases, thus leading to longer relaxation times and hence broader lines in the Mössbauer spectrum.[32]

Other workers have shown that the sign of the electronic field gradient and hence the sign of the quadrupole splitting may be determined from an examination of the asymmetry of the Mössbauer line shape, the higher-energy component of the spectrum (transition $\pm\frac{3}{2} \longrightarrow \pm\frac{1}{2}$) collapsing first in the presence of a fluctuating magnetic field if the sign of the quadrupole splitting is positive.[33] Yamauchi *et al.*[34] have shown, using the point-charge model, that the sign of the quadrupole splitting may be correlated to the magnitude of the *cis*-O–Fe–O bond angle, being positive for values <90° and negative for those >90°.

The Fe–Fe distance found in $[FeL_3]$ is 8.6 Å which is comparable to those in those tris(β-diketonato)iron(III) complexes which exhibit line broadening due to partial spin–spin relaxation, *e.g.* 7.6 Å for tris(acetylacetonato)iron(III).[22] It can therefore be expected that the ^{57}Fe Mössbauer spectrum of $[FeL_3]$ should also display broad lines due to these effects.

By examination of the spectra it can be observed that the higher-energy component of the spectrum becomes much more pronounced at higher temperatures. From this we conclude that the sign of the electric field gradient and hence the sign of the quadrupole splitting (the two being the same for ^{57}Fe Mössbauer spectroscopy) is positive. This is in good agreement with the proposal of Yamauchi *et al.* since the *cis*-O–Fe–O bond angle for $[FeL_3]$ is less than 90° (mean 80.5°), although for five- and six-membered chelate rings the angles must always be less than 90° if the ligating atoms are oxygens.

Conclusions

The crystal structure data for [FeL$_3$] and the other complexes in Table 3 can be used to show the pitfalls of overinterpretation. Packing forces and interligand repulsion forces play an important role in dictating the geometry around the iron(III) centre in a tris chelate iron(III) complex. However, if the ligand is not symmetrical (such as maltol in this case), then some evidence of this in the Fe–O bonding can be found by comparing this structure to that of other relevant structures (Table 3). The optimum way to study such effects using single-crystal *X*-ray diffraction studies is by comparing several similar asymmetrical structures. It is nevertheless possible to state from this work that the presence of asymmetric aromatic rings (as part of chelating ligands) will have a significant effect on the bonding at the chelation centre. However, before more useful information on factors that may influence the iron binding can be obtained from these data and those of the other known iron structures, more structures of tris chelate iron(III) complexes containing specifically substituted asymmetric aromatic rings must be determined. When such data become available, it should be possible to optimize ligand design to maximize properties such as stability constants.

Experimental

mer-Tris(3-hydroxy-2-methyl-4*H*-pyran-4-onato)iron(III) was prepared using a method not previously described. 3-Hydroxy-2-methyl-4*H*-pyran-4-one (3.78 g, 0.03 mol) and anhydrous iron(III) chloride (1.62 g, 0.01 mol) were dissolved in ethanol–water (1:1, 200 cm^3). The pH of the solution was raised to 7.5 using an ammonia solution, followed by stirring for 1 h. After this time the ethanol was removed *in vacuo* and the complex extracted into chloroform. The chloroform was removed *in vacuo* to yield the solid product which was a deep wine red in colour. Crystals were obtained by the slow evaporation of an almost saturated solution in chlorobenzene (Found: C, 50.0; H, 3.5; Fe, 13.0. Calc. for $C_{18}H_{15}FeO_9$: C, 50.1; H, 3.5; Fe, 12.9%).

^{57}Fe *Mössbauer Spectroscopy*.—^{57}Fe Mössbauer spectra were recorded on an instrument previously described.[35] Absorbers were prepared using a sample concentration of 10 mg Fe cm^{-2} diluted in Al_2O_3. The instrument was calibrated using natural iron foil and all shifts are referred to this as zero velocity.

Structure Determination.[36]—*Crystal data*. $C_{18}H_{15}FeO_9$, M = 431.2, monoclinic, space group $P2_1/c$, a = 7.369(1), b = 14.720(3), c = 19.964(5) Å, β = 100.41(2)°, U = 2 098.1 Å^3, Z = 4, D_c = 1.36 g cm^{-3}, Mo-K_α radiation (graphite monochromated), λ = 0.710 69 Å, μ(Mo-K_α) = 7.07 cm^{-1}, F(000) = 884.

Data were measured on an Enraf-Nonius CAD-4 diffractometer using a crystal of dimensions *ca.* 0.25 × 0.25 × 0.4 mm. Final unit-cell dimensions and standard deviations were calculated by a least-squares refinement of the setting angles of a series of reflections with $\theta \approx 15°$. Intensities for reflections $h, k, \pm l$ with $1.5 < \theta < 25.0°$ were measured by the ω–2θ scan technique with a scan width $\Delta\theta(0.8 \pm 0.35 \tan\theta)°$. The intensities of three reflections, (0, 8, 0), (0, 4, −8), and (3, 0, 10), were measured approximately every 100 reflections, however these showed no significant change over the duration of the data collection. Equivalent reflections were averaged to give 3 687 unique reflections out of a possible 4 148. 952 Reflections with $F_o < 3\sigma(F_o)$ were considered 'unobserved' and a total of 2 735 reflections were used in the refinement. The data were corrected for Lorentz and polarization effects but not for absorption since μ(Mo-K_α) = 7.07 cm^{-1}. Systematic absences $k\,0\,l, l \neq 2n$ indicated space group $P2_1/c$, no. 14.[37]

The positional parameters of the iron atom in the asymmetric unit were determined from a three-dimensional Patterson synthesis. Subsequent Fourier difference syntheses revealed the positional parameters of the remaining non-hydrogen atoms. Full-matrix least-squares refinement of the positional parameters and anisotropic thermal parameters using the program SHELX 76[38] gave R = 0.081. A difference electron-density synthesis calculated at this stage revealed small positive peaks in the positions expected for H atoms and these were included in the final cycles of refinement (U = 0.08 Å^2). The largest peaks remaining on a final Fourier difference synthesis were of height 1.4—1.6 e Å^{-3} at positions around $x, \frac{1}{2}, \frac{1}{2}$. Although no chemically significant information could be concluded from them they could be due to either a very disordered solvent molecule lying in a channel parallel to the a axis or termination errors. A weighting scheme of the form $w = 1/[\sigma^2(F) + gF^2]$ with g = 0.0026 was used and found to be satisfactory. Final R = 0.0649, $R' = [\Sigma w(|F_o| - |F_c|)^2/\Sigma w|F_o|^2]^{\frac{1}{2}}$ = 0.0718. The maximum value of the shift-to-error ratio was 0.076 (mean 0.017). Atomic scattering factors were taken from ref. 39. The final value of $S = [\Sigma w(|F_o| - |F_c|)^2/(N_F - N_P)]^{\frac{1}{2}}$ = 1.6638 where N_F = number of reflections and N_P = number of parameters.

Calculations were performed either on the University of Essex DEC PDP-10 or the McMaster University VAX8600 computer. Final atomic co-ordinates are given in Table 1.

Additional material available from the Cambridge Crystallographic Data Centre comprises H-atom co-ordinates and thermal parameters.

Acknowledgements

J. S. thanks the S.E.R.C. for a crystal data collection allocation and the staff at Queen Mary College Crystallographic Unit for their assistance. The authors thank Professor T. Birchall for the use of liquid helium facilities.

References

1 T. H. Bothwell, R. W. Charlton, T. D. Cook, and C. A. Finch (eds.), 'Iron Metabolism in Man,' Blackwell Scientific Publications, Oxford, 1979.

2 D. A. Brown, M. V. Chidambaram, J. J. Clarke, and D. M. McAleese, *Bioinorg. Chem.*, 1978, **9**, 255.

3 R. C. Hider, G. Kontioghiorghes, J. Silver, and M. A. Stockham, B.P. Appl. G.B. 2 117 766/1983 (*Chem. Abstr.*, 1984, **101**, 23339K).

4 R. C. Hider, G. Kontioghiorghes, and M. A. Stockham, Eur.P. Appl. E.P. 107 458/1984 (*Chem. Abstr.*, 1984, **101**, 71603p).

5 R. C. Hider, G. Kontioghiorghes, J. Silver, and M. A. Stockham, B.P. Appl. G.B. 2 136 807/1984 (*Chem. Abstr.*, 1985, **102**, 113301s).

6 R. C. Hider, G. Kontioghiorghes, J, Silver, and M. A. Stockham, B.P. Appl. G.B. 213 806/1985 (*Chem. Abstr.*, 1985, **102**, 113302t).

7 R. C. Hider, G. Kontioghiorghes, J. Silver, and M. A. Stockham, Eur. P. Appl. E.P. 138 421/1985 (*Chem. Abstr.*, 1985, **103**, 196001p).

8 R. C. Hider, G. Kontioghiorghes, J. Silver, and M. A. Stockham, Eur. P. Appl. E.P. 138 420/1985 (*Chem. Abstr.*, 1985, **103**, 196002q).

9 C. Gerard and R. R. Hugel, *J. Chem. Res.*, 1980, (*M*), 3919.

10 G. Kontioghiorghes, Ph.D. Thesis, University of Essex, 1982.

11 A. Stefanovic, J. Havel, and L. Sommer, *Collect. Czech. Chem. Commun.*, 1968, **33**, 4198.

12 C. Gerard, *Bull. Soc. Chim. Fr.*, 1979, **11**—**12**, 451.

13 Pfizer Technical Bulletin, Pfizer Chemicals Corp., Sandwich, Report C155, 1984.

14 E. J. Gralla, R. B. Stebbins, G. L. Coleman, and C. S. Delahunt, *Toxicol. Appl. Pharmacol.*, 1969, **15**, 604.

15 C. Johnson, ORTEP, A Fortran Thermal Ellipsoid Program, O.R.N.L., Oak Ridge, Tennessee, 1965.

16 M. M. Finnegan, S. J. Rettig, and C. Orvig, *J. Am. Chem. Soc.*, 1986, **108**, 5033.

17 B. F. Anderson, D. A. Buckingham, G. B. Robertson, and J. Webb, *Acta Crystallogr., Sect. B*, 1982, **38**, 1927.

18 K. N. Raymond, S. S. Isied, L. D. Brown, F. R. Fronczek, and J. H. Nibert, *J. Am. Chem. Soc.*, 1976, **98**, 1767.
19 B. F. Anderson, J. Webb, D. A. Buckingham, and G. B. Robertson, *J. Inorg. Biochem.*, 1982, **16**, 21.
20 L. S. White, P. V. Nilsson, L. H. Pignolet, and L. Que, jun., *J. Am. Chem. Soc.*, 1984, **106**, 8312.
21 D. A. Buckingham, C. R. Clark, M. G. Weller, and G. F. Gainsfond, *J. Chem. Soc., Chem. Commun.*, 1982, 779.
22 J. Iball and C. H. Morgan, *Acta Crystallogr.*, 1967, **23**, 239.
23 L. R. Nassimbeni and M. M. Thackeray, *Acta Crystallogr., Sect. B*, 1974, **30**, 1072.
24 T. A. Hamor and D. J. Watkin, *Chem. Commun.*, 1969, 440.
25 R. C. Scarrow, P. E. Riley, K. Abu-Dari, D. L. White, and K. N. Raymond, *Inorg. Chem.*, 1985, **24**, 954.
26 D. L. Kepert, *Inorg. Chem.*, 1982, **11**, 1561.
27 I. D. Brown and D. Altermatt, *Acta Crystallogr., Sect. B*, 1985, **41**, 244.
28 I. D. Brown, *Chem. Soc. Rev.*, 1978, **7**, 359.
29 M. Blume, *Phys. Rev. Lett.*, 1965, **14**, 96.
30 M. Blume, *Phys. Rev. Lett.*, 1967, **18**, 305.
31 M. Cox, B. W. Fitzsimmons, A. W. Smith, L. F. Larkworthy, and K. A. Rogers, *Chem. Commun.*, 1969, 183.
32 J. W. G. Wignall, *J. Chem. Phys.*, 1966, **44**, 2463.
33 G. M. Bancroft, A. G. Maddock, W. K. Ong, R. H. Prince, and A. J. Stone, *J. Chem. Soc. A*, 1967, 1966.
34 S. Yamauchi, Y. Sakai, and T. Tominaga, *Bull. Chem. Soc. Jpn.*, 1985, **58**, 442.
35 M. Y. Hamed, R. C. Hider, and J. Silver, *Inorg. Chim. Acta*, 1982, **66**, 13.
36 M. R. Hursthouse, R. A. Jones, K. M. Abdul Malik, and G. Wilkinson, *J. Am. Chem. Soc.*, 1979, **101**, 4128.
37 'International Tables for *X*-Ray Cyrstallography,' Kynoch Press, Birmingham, 1985, vol. 1.
38 G. M. Sheldrick, SHELX 76, Program for Crystal Structure Determinations, University of Cambridge, 1976.
39 D. T. Cromer and J. B. Mann, *Acta Crystallogr., Sect. A*, 1968, **24**, 321.

Received 8th *June* 1987; *Paper* 7/1007